COUPLED NON-NEGATIVE MATRIX FACTORIZATION (CNMF) FOR HYPERSPECTRAL AND MULTISPECTRAL DATA FUSION: APPLICATION TO PASTURE CLASSIFICATION

Naoto Yokoya,[1] *Takehisa Yairi,*[2] *and Akira Iwasaki*[2]

[1]Department of Aeronautics and Astronautics, The University of Tokyo, Japan
[2]Research Center for Advanced Science and Technology, The University of Tokyo, Japan

ABSTRACT

Coupled non-negative matrix factorization (CNMF) is introduced for hyperspectral and multispectral data fusion. The CNMF fused data have little spectral distortion while enhancing spatial resolution of all hyperspectral band images owing to its unmixing based algorithm. CNMF is applied to the synthetic dataset generated from real airborne hyperspectral data taken over pasture area. The spectral quality of fused data is evaluated by the classification accuracy of pasture types. The experiment result shows that CNMF enables accurate identification and classification of observed materials at fine spatial resolution.

Index Terms— Non-negative matrix factorization, unmixing, data fusion, pasture classification

1. INTRODUCTION

The spatial resolution of hyperspectral sensors is often lower than that of multispectral sensors. The hyperspectral and multispectral mission named HISUI (Hyperspectral Imager Suite) is the Japanese next-generation spaceborne radiometer [1]. HISUI is composed of a hyperspectral radiometer with 30 m ground sampling distance (GSD) and 186 spectral channels over 400-2500 nm, and a multispectral radiometer with 5 m GSD and 4 spectral channels over 450-900 nm. Data fusion of hyperspectral and multispectral data has a possibility of producing fused data with both higher spatial and spectral resolutions, which contribute to the accurate identification and classification of observed materials at fine spatial resolution.

In low-spatial-resolution hyperspectral data, an observed spectrum at each pixel is a mixture of several endmember spectra, and is commonly called as "mixel" (mixed pixel). Unmixing is a technique to decompose the observed spectrum into endmember spectra and their abundance fractions. In the recent decade, non-negative matrix factorization (NMF) [2], [3], has become one of the most useful hyperspectral unmixing techniques based on a linear spectral mixture model [4]-[6]. Given a non-negative matrix $\mathbf{V}$, NMF looks for two non-negative matrix factors $\mathbf{W}$ and $\mathbf{H}$ such that $\mathbf{V} = \mathbf{WH}$. When NMF is applied to hyperspectral unmixing, $\mathbf{V}$, $\mathbf{W}$, and $\mathbf{H}$ correspond to observed data, endmember spectra, and abundance fractions, respectively.

We proposed coupled non-negative matrix factorization (CNMF) for the fusion of spectroradiometer datasets [7]. In the case of hyperspectral and multispectral data fusion, CNMF unmixes the low-spatial-resolution hyperspectral data and the high-spatial-resolution multispectral data alternately using the relation between sensor properties for the NMF initializations. By combining the hyperspectral endmember matrix and the high-spatial-resolution abundance matrix, high-spatial-resolution hyperspectral data that inherit both advantages of the two data can be synthesized. The CNMF method is physically straightforward and easy to implement, owing to its simple update rules. Since CNMF is based on spectral unmixing, the CNMF fused data have little spectral distortion while enhancing spatial resolution of all hyperspectral band images.

In this work, we introduce the CNMF algorithm for hyperspectral and multispectral data fusion and investigate the utility of the fused data for pasture classification. CNMF is applied to the synthetic dataset generated from real airborne hyperspectral data taken over pasture area. After numerical evaluation of the spatial and spectral qualities of the fused data, its utility for pasture classification is demonstrated.

2. COUPLED NON-NEGATIVE MATRIX FACTORIZATION (CNMF)

The aim of hyperspectral and multispectral data fusion is to estimate unobservable high-spatial-resolution hyperspectral data ($\mathbf{Z} \in \mathbb{R}^{\lambda_h \times L_m}$) from observable low-spatial-resolution hyperspectral ($\mathbf{X} \in \mathbb{R}^{\lambda_h \times L_h}$) and multispectral ($\mathbf{Y} \in \mathbb{R}^{\lambda_m \times L_m}$) data, which are spatially co-registered. Here, λ_h and λ_m denote the numbers of spectral channels of hyperspectral and multispectral sensors, respectively. L_h and L_m denote the numbers of pixels of hyperspectral and multispectral data, respectively. $\lambda_h > \lambda_m$ and $L_h < L_m$ are satisfied due to the trade-off between spatial and spectral resolutions of two sensors.

2.1. Observation Model

The relation between the low- and high-spatial-resolution hyperspectral data can be expressed in matrix form by

$$\mathbf{X} = \mathbf{Z}\mathbf{S} + \mathbf{N}_s, \tag{1}$$

where $\mathbf{S} \in \mathbb{R}^{L_m \times L_h}$ is the spatial transform matrix with each column vector $\{\mathbf{s}_k\}_{k=1}^{L_h}$ representing the transform from the point spread function of the high-spatial-resolution hyperspectral data to that of k th pixel value in the low-spatial-resolution hyperspectral data. $\mathbf{N}_s$ is the residual error. Similarly, the multispectral data is related to the high-spatial-resolution hyperspectral data by

$$\mathbf{Y} = \mathbf{R}\mathbf{Z} + \mathbf{N}_r, \tag{2}$$

where $\mathbf{R} \in \mathbb{R}^{\lambda_m \times \lambda_h}$ is the spectral transform matrix with each row vector $\{\mathbf{r}_i\}_{i=1}^{\lambda_m}$ representing the transform from the spectral response function of the hyperspectral data to the i th band in the multispectral data. $\mathbf{N}_r$ denotes the residual error. In the simulation of this work with synthetic data, $\mathbf{S}$ and $\mathbf{R}$ are given.

When applied to real data, $\mathbf{S}$ is determined by image registrations and estimation of point spread functions and $\mathbf{R}$ is derived from radiometric calibration to obtain spectral response functions.

2.2. Coupled NMF Unmixing

With the linear spectral mixture assumption, $\mathbf{X}$ and $\mathbf{Y}$ are expressed as follows:

$$\mathbf{X} = \mathbf{W}_h\mathbf{H}_h + \mathbf{E}_h, \tag{3}$$

$$\mathbf{Y} = \mathbf{W}_m\mathbf{H}_m + \mathbf{E}_m. \tag{4}$$

Here, $\mathbf{W}_h \in \mathbb{R}^{\lambda_h \times D}$, $\mathbf{H}_h \in \mathbb{R}^{D \times L_h}$, and $\mathbf{E}_h \in \mathbb{R}^{\lambda_h \times L_h}$ are the endmember, abundance, and residual matrices of the low-spatial-resolution hyperspectral data, respectively. $\mathbf{W}_m \in \mathbb{R}^{\lambda_m \times D}$, $\mathbf{H}_m \in \mathbb{R}^{D \times L_m}$, and $\mathbf{E}_m \in \mathbb{R}^{\lambda_m \times L_m}$ are those of the multispectral data. NMF spectral unmixing is commonly performed to minimize the squared Frobenius norm of the residual matrix in the linear spectral mixture model expressed as $\|\mathbf{E}_h\|_F^2$ and $\|\mathbf{E}_m\|_F^2$ for (3) and (4), respectively. Lee and Seung proposed a multiplicative update rule (MUR) that is guaranteed to converge to a locally optima under the non-negativity constraints of factorized two matrices. We used MUR for NMF unmixings of $\mathbf{X}$ and $\mathbf{Y}$. It is physically reasonable to assume that the high-spatial-resolution hyperspectral data contains the same endmember spectra as the low-spatial-resolution hyperspectral data and the same abundance maps as the multispectral data. Therefore, $\mathbf{Z}$ can be approximated as

$$\mathbf{Z} \approx \mathbf{W}_h\mathbf{H}_m. \tag{5}$$

This is the key idea of CNMF data fusion. From (1)-(4) and (5), the endmember and abundance matrices are related as

$$\mathbf{H}_h \approx \mathbf{H}_m\mathbf{S}, \tag{6}$$

$$\mathbf{W}_m \approx \mathbf{R}\mathbf{W}_h. \tag{7}$$

CNMF alternately unmixes $\mathbf{X}$ and $\mathbf{Y}$ to estimate $\mathbf{W}_h$ and $\mathbf{H}_m$ under constraints of (6) and (7).

The CNMF algorithm starts from NMF of $\mathbf{X}$ to use its spectral advantage. As the initialization phase, with the number of endmembers D set to a certain value, $\mathbf{W}_h$ is initialized by vertex component analysis (VCA), which is one of the most advanced geometry based endmember extraction methods with pure pixel assumption. $\mathbf{H}_h$ is set to a constant value $1/D$ and updated by MUR with $\mathbf{W}_h$ fixed. As the optimization phase, $\mathbf{W}_h$ and $\mathbf{H}_h$ are updated by MUR until convergence. In the subsequent rounds, only the initialization phase is different, i.e., the value of $\mathbf{H}_h$ that is initialized by (6) is used and $\mathbf{W}_h$ is updated by MUR with $\mathbf{H}_h$ fixed to inherit the reliable abundance information obtained from NMF of $\mathbf{Y}$.

The alternate step of CNMF is NMF of $\mathbf{Y}$. As the initialization phase, $\mathbf{W}_m$ is initialized by (7). $\mathbf{H}_m$ is set to a constant value $1/D$ and updated by MUR with $\mathbf{W}_m$ fixed to inherit the reliable endmember spectra obtained from NMF of $\mathbf{X}$. As the optimization phase, $\mathbf{W}_m$ and $\mathbf{H}_m$ are updated by MUR until convergence.

We refer to the alternate NMF unmixings as the outer loops and the update processes in each NMF nimxing as the inner loops. As a convergence condition, we use the condition that the change ratio of cost function achieves a value below a given threshold. Considering practical use, a maximum number of iterations is set for each loop. Two parameters are set for the outer and inner loops, respectively, as different values.

3. EXPERIMENT

3.1. Dataset

CNMF is applied to the synthetic dataset generated from compact airborne spectrographic imager 3 (CASI-3) data taken over pasture area in Hokkaido, Japan, on June 19, 2009. The original data have 34 spectral channels over 410-1070 nm with 1 m GSD. The data, originally measured as radiance, was converted into reflectance. By down-sampling the original high-spatial-resolution hyperspectral data in the spectral and spatial domains, we generate the synthetic dataset simulating the characteristics of HISUI except for spectral resolution of hyperspectral sensor. We ideally assume rectangle functions for the point spread and spectral response functions of two sensors. The multispectral data are produced by averaging 5×5 pixel blocks of the original data with uniform spectral response functions corresponding to the multispectral bands 1-4 of the HISUI, which cover the 450-520, 520-600, 630-690, and 760-900 nm regions, respectively. The
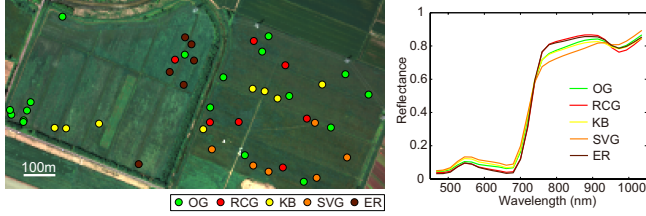
Fig. 1. (a) RGB color image of test area with ground truth classification samples plotted and (b) spectra of five plants.

Table 1. SAD (deg) between five plants.

	OG	RCG	KB	SVG	ER
OG	0	2.688	1.008	2.892	2.324
RCG		0	3.266	5.518	0.906
KB			0	2.516	2.956
SVG				0	5.088
RE					0

low-spatial-resolution hyperspectral data are generated by averaging 30×30 pixel blocks of the original data. In the same way, we made the hyperspectral data with 5 m GSD as the reference data that we aim to produce by CNMF.

3.2. Evaluation of fused data

The qualities of the CNMF fused data are evaluated by comparing it with the reference data. Peak-signal-to-noise ratio (PSNR) is used to evaluate the spatial reconstructivity of each band image. Higher PSNR indicates better spatial reconstructivity. Brovey transform, which is one of the most popular pan-sharpen algorithms, is used as the comparison method. This method is applicable only for spectral regions covered by the multispectral sensor. For each pixel spectrum, spectral angle distance (SAD) is used to evaluate the spectral distortion. Smaller SAD indicates less spectral distortion.

3.3. Classification

The utility of the CNMF fused data for classification is evaluated by pasture classification. Observed pasture is mainly composed of five plants such as orchard grass (OG), reed canary grass (RCG), Kentucky bluegrass (KB), sweet vernal grass (SVG), and Elytrigia repens (ER). Ground truth data, i.e., class labels and spectra, were obtained at 45 quadrate areas with 3×3 m size. Analytical Spectral Device (ASD) FieldSpec Pro spectroradiometer was used for field spectrum measurement. Fig. 1 shows the RGB color image of the test area with ground truth classification samples superposed and the spectra of the five plants. SAD between these spectra are summarized in Table 1. Pairs of OG and KB, and RCG and ER are spectrally similar with about one degree of SAD. Since
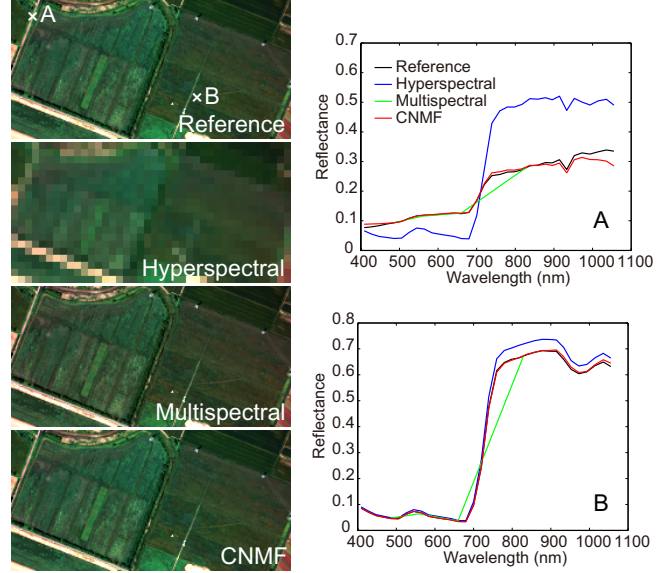

Fig. 2. (a) Endmember spectra and continuum removed spectra in (b) 545-760 nm and (c) 900-1035 nm.

the CASI data have a geometrical error of about 2 m, the classification result is considered as correct if the major plant in a 3×3 pixel square with its center set within 2 m of the sampling point matches the ground truth data. We use the spectral angle mapper (SAM) as a classifier. Especially for the hyperspectral data, the continuum removal method with the 545-760 nm and 900-1035 nm regions is adopted [8]. Classification accuracy of the CNMF fused data is compared with those of the hyperspectral, multispectral, and reference data.

4. RESULTS AND DISCUSSION

Left images of Fig. 2 show RGB image of the CNMF fused data with those of the reference, hyperspectral, and multispectral data. Right graphs show the comparison of spectra at two points. The CNMF fused data is close to the reference data both in terms of spatial and spectral domains. Fig. 3 (a) shows the PSNR of the fused data obtained by CNMF and Brovey. CNMF outperforms Brovey in all spectral bands owing to its unmixing based optimization algorithm. In the spectral bands not covered by multispectral data, the PSNR values of the CNMF fused data are relatively low. This indicates that resolution enhancement is limited without high-spatial-resolution information. Fig. 3 (b) and (c) show the histogram of SAD and the SAD distribution map, respectively. In a lot of vegetation areas, SAD is around one degree, which is comparable with the minimum SAD between five plants. Streams and trails show larger SAD. Since there are no pure pixels of these objects in the low-spatial-resolution hyperspectral data, it is difficult to retrieve their endmember spectra by NMF un-
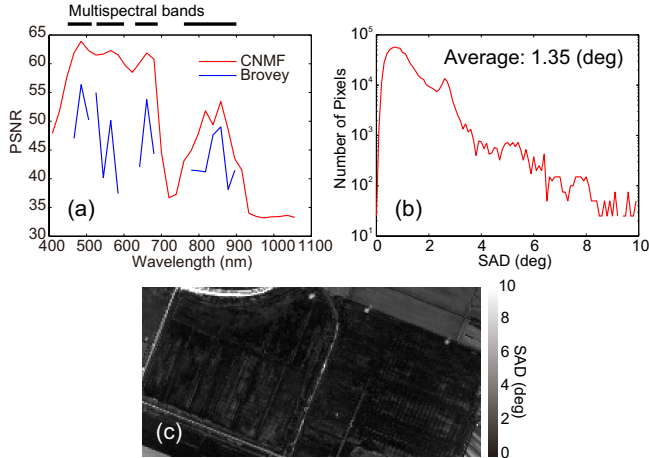
Fig. 3. (a) PSNR, (b) histogram of SAD, and (c) SAD distribution map.

Fig. 4. Classification of pasture types generated from four data, i.e., the (a) hyperspectral, (b) multispectral, (c) CNMF, and (d) reference data.

mixing. Spectra of water and soil can not be expressed as linear combinations of vegetation spectra, which results in larger SAD. To produce fused data with little spectral distortion, endmember extraction is the most important process.

Fig. 4 shows the classification result of the observed area and Table 2 shows classification accuracies for four data, i.e., the hyperspectral, multispectral, CNMF, and reference data. Low classification accuracies of the hyperspectral and multispectral data suggest that both spatial and spectral resolutions have significant effects on accurate classification. The CNMF fused data shows comparable classification accuracy with the reference data, outperforming the hyperspectral and multispectral data. This indicates that the CNMF method has a potential to produce high-spatial-resolution hyperspectral data with little spectral distortion that enable accurate identification and classification of observed materials at fine spatial resolution.

Table 2. Classification accuracies (%) for four data.

Hyperspectral	Multispectral	CNMF	Reference
46.7	51.1	64.4	66.7

6. ACKNOWLEDGMENT

5. CONCLUSION

In this work, we introduced CNMF for hyperspectral and multispectral data fusion and demonstrated its utility for accurate classification. Two data with trade-off between spatial and spectral resolutions are reshaped as matrices and unmixed into endmember and abundance matrices by NMF. By multiplying the endmember matrix derived from hyperspectral data unmixing and the high-spatial-resolution abundance matrix derived from multispectral data unmixing, high-spatial-resolution hyperspectral data can be obtained. CNMF is applied to the synthetic dataset generated from CASI data taken over pasture areas. Classification experiment of pasture types proved that CNMF fused data enable accurate identification and classification of observed materials at fine spatial resolution. This technique is useful for the generation of higher-order data products in the HISUI dataset.
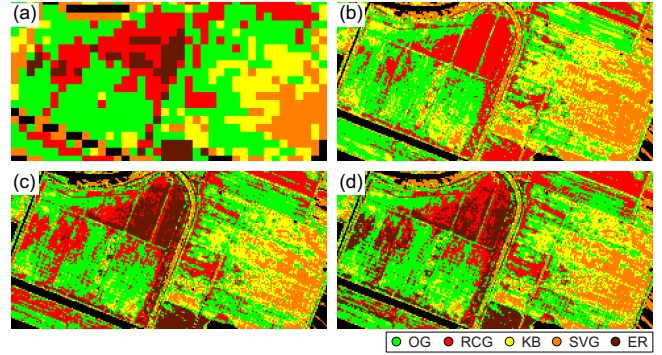
7. REFERENCES

[1] N. Ohgi, A. Iwasaki, T. Kawashima, and H. Inada, "Japanese hyper-multi spectral mission," in *Proc. IEEE IGARSS*, Jul. 2010, pp. 3756-3759.

[2] D. D. Lee and H. S. Seung, "Learning the parts of objects by nonnegative matrix factorization," *Nature*, vol. 401, pp. 788-791, Oct. 1999.

[3] D. D. Lee and H. S. Seung "Algorithms for non-negative matrix factorization," in *Proc. Conf. Adv. Neural Inf. Process. Syst.*, 2001, vol. 13, pp. 556-562.

[4] L. Miao and H. Qi, "Endmember extraction from highly mixed data using minimum volume constrained nonnegative matrix factorization," *IEEE Trans. Geosci. Remote Sens.*, vol. 45, no. 3, pp. 765-777, Mar. 2007.

[5] S. Jia and Y. Qian, "Constrained nonnegative matrix factorization for hyperspectral unmixing," *IEEE Trans. Geosci. Remote Sens.*, vol. 47, no. 1, pp. 161-173, Jan. 2009.

[6] A. Huck, M. Guillaume, and J. Blanc-Talon, "Minimum dispersion constrained nonnegative matrix factorization to unmix hyperspectral data," *IEEE Trans. Geosci. Remote Sens.*, vol. 48, no. 6, pp. 2590-2602, Jun. 2010.

[7] N. Yokoya, T. Yairi, and A. Iwasaki, "Hyperspectral, multispectral, and panchromatic data fusion based on coupled non-negative matrix factorization," in *Proc. IEEE WHISPERS*, Lisbon, Jun. 2011.

[8] ERSDAC, "Annual report in the research and development of usage technology for the next generation advanced earth observing satellite," (in Japanese), pp. 47-51, Mar. 2010.